



MSU Graduate Theses

Fall 2022

Testing the Impact of a Silencing Suppressor on Infectivity of Grapevine Vein Clearing Virus Infectious Clone in *Nicotiana Benthamiana*

Wen Zhao

Missouri State University, Zhao0723@live.missouristate.edu

As with any intellectual project, the content and views expressed in this thesis may be considered objectionable by some readers. However, this student-scholar's work has been judged to have academic value by the student's thesis committee members trained in the discipline. The content and views expressed in this thesis are those of the student-scholar and are not endorsed by Missouri State University, its Graduate College, or its employees.

Follow this and additional works at: <https://bearworks.missouristate.edu/theses>

 Part of the [Plant Pathology Commons](#)

Recommended Citation

Zhao, Wen, "Testing the Impact of a Silencing Suppressor on Infectivity of Grapevine Vein Clearing Virus Infectious Clone in *Nicotiana Benthamiana*" (2022). *MSU Graduate Theses*. 3816.
<https://bearworks.missouristate.edu/theses/3816>

This article or document was made available through BearWorks, the institutional repository of Missouri State University. The work contained in it may be protected by copyright and require permission of the copyright holder for reuse or redistribution.

For more information, please contact BearWorks@library.missouristate.edu.

**TESTING THE IMPACT OF A SILENCING SUPPRESSOR ON INFECTIVITY OF
GRAPEVINE VEIN CLEARING VIRUS INFECTIOUS CLONE IN *NICOTIANA*
*BENTHAMIANA***

A Master's Thesis

Presented to

The Graduate College of
Missouri State University

In Partial Fulfillment

Of the Requirements for the Degree
Master of Science, Plant Science

By

Wen Zhao

December 2022

Copyright 2022 by Wen Zhao

**TESTING THE IMPACT OF A SILENCING SUPPRESSOR ON INFECTIVITY OF
GRAPEVINE VEIN CLEARING VIRUS INFECTIOUS CLONE IN *NICOTIANA
BENTHAMIANA***

William H. Darr College of Agriculture

Missouri State University, December 2022

Master of Science

Wen Zhao

ABSTRACT

Grapevine vein clearing virus (GVCV), the first DNA virus of the Badnavirus genus discovered in grapevines, is closely associated with grapevine vein-clearing disease. Through earlier research, Koch's postulates were partially met: GVCV was in all diseased plants; GVCV was introduced into a healthy grapevine through grafting and by aphids and caused the disease. However, more shreds of evidence are required to fulfill the last postulate, the same virus must be reisolated from the inoculated diseased grapevine (1). A full-length infectious clone of GVCV was previously constructed to provide evidence; however, its infectivity was not consistent. Therefore, the goal of this thesis research was to increase infectivity. I hypothesized that the low infectivity of GVCV infectious clones is due to virus-induced gene silencing (VIGS) in host plants. It is known that P19 of tomato bushy stunt virus (TBSV) is a viral suppressor of VIGS. I tested the hypothesis by adding TBSV P19 to the agroinfection. I used the agrobacterial strain GV3101 as control, as well as GV3101-LBC, which carries the 1.4 GVCV genome, At-pKYLX7-P19, and At-pKYLX7-GFP. The polymerase chain reaction (PCR) was used for GVCV detection and real-time quantitative PCR was used for qualifying the number of GVCV genomes in plant tissue. The results showed that GVCV effectively infected *N. benthamiana*. The GVCV genome number was not statistically different in the plants that were agroinfected with GVCV infectious clones with or without the addition of TBSV P19. Therefore, there was insufficient evidence to support that P19 can improve the infectivity of the GVCV infectious clone.

KEYWORDS: *grapevine vein clearing virus*, infectious clone, virus-induced gene silencing, P19, agroinfiltration

**TESTING THE IMPACT OF A SILENCING SUPPRESSOR ON INFECTIVITY OF
GRAPEVINE VEIN CLEARING VIRUS INFECTIOUS CLONE IN *NICOTIANA*
*BENTHAMIANA***

By

Wen Zhao

Master of Science, Plant Science

A Master's Thesis
Submitted to the Graduate College
Of Missouri State University
In Partial Fulfillment of the Requirements
For the Degree of Master of Science, Plant Science

December 2022

Approved:

Wenping Qiu, Ph.D., Thesis Committee Chair

Chin-Feng Hwang, Ph.D., Committee Member

Melissa A. Bledsoe, Ph.D., Committee Member

Julie Masterson, Ph.D., Dean of the Graduate College

In the interest of academic freedom and the principle of free speech, approval of this thesis indicates the format is acceptable and meets the academic criteria for the discipline as determined by the faculty that constitute the thesis committee. The content and views expressed in this thesis are those of the student-scholar and are not endorsed by Missouri State University, its Graduate College, or its employees.

ACKNOWLEDGEMENTS

In the two years of my academic career, I realized that scientific research and writing a thesis are not easy things. It requires patience, care, innovation, research, logic, and a good mind. These two years have changed my life. First of all, I would like to thank all the members of the laboratory for their teaching and help.

This paper was completed under the supervision Dr. Wenping Qiu. He used his deep academic background, patient attitude, and encouraging teaching to help me complete the experiments and thesis. As the "father" of our laboratory, he has great enthusiasm and a rigorous attitude toward biological science, which deeply influenced me. What's more, he has the desire to pursue truth and love for students. He not only pays attention to our experimental progress but also cares about our life. Thank you for giving me this opportunity to be your student, You're an amazing teacher!

Sylvia, you are the best lab manager I've ever seen, you're the mother of our lab. Your patience and love helped me to complete the experiment. You are my best English teacher, you are the first person I think of when I have trouble in school. Thank you for your two and a half years of infinite help to me. Your love for career and maintenance of family affect me. You are the best model for female growth, and you help me more than just in the academic field. But I want to be a rigorous scientific researcher like you, and also a great patient mother.

Matthew, thank you so much for watering my baby plant when I was busy. I will miss the time we take classes together and spend time in the lab together.

Then I want to thank my family. Thank you for supporting me to study abroad and giving me unlimited spiritual encouragement, respect, and understanding. Also, I'd like to thank my boyfriend Yufei, Duan. I appreciate your appearing in my life at the beginning of my thesis. Your self-discipline and hard-working on academic career are encouraging me imperceptibly. Your excellence makes me want to strive to be a better person. Thank you for making me full of motivation and joy in the process of writing this thesis.

Finally, I would like to thank my committee member, Dr. Hwang, and Dr. Bledsoe, for your patience and kindness in helping me to graduate successfully.

TABLE OF CONTENTS

Introduction	1
Literature Review	4
Badnavirus	4
Grapevine vein clearing virus	6
Infectious clone	9
Agroinoculation	10
Silence suppressor	12
Well-studied infectious clones of grapevine viruses	15
Methods	19
<i>Nicotiana benthamiana</i> plants	19
Agrobacterial strains and treatment for agroinfiltration	19
Agroinfiltration of <i>Nicotiana benthamiana</i> plants	20
Culturing of agrobacteria strains	21
Agroinfiltration of <i>Nicotiana benthamiana</i> plants	21
DNA extraction from <i>Nicotiana benthamiana</i> leaves	22
Polymerase chain reaction (PCR)	23
Quantitative polymerase chain Reaction (qPCR)	24
Standard curve	25
Results	28
Testing infectivity of GVCV infectious clone on <i>Nicotiana benthamiana</i> by PCR.	28
Demonstration of TBSV P19's effect on the GFP expression in <i>Nicotiana benthamiana</i>	29
Analysis of GVCV genome molecules in agroinfiltrated <i>Nicotiana benthamiana</i> by Real-Time Quantitative PCR	30
Discussion	32
References	36

LIST OF TABLES

Table 1. Primers used for detecting Grapevine vein clearing virus and assessing DNA quality	Page 41
Table 2. Experimental design for testing the impact of Tomato bushy stunt virus (TBSV) P19 on the infectivity of GVCV infectious clone on <i>N. benthamiana</i>	Page 42
Table 3. Presence of GVCV in agroinfiltrated <i>N. benthamiana</i> plants	Page 43

LIST OF FIGURES

Figure 1. Typical symptoms of a Chardonnay grapevine that was infected by GVCV.	Page 44
Figure 2. Testing of GVCV replication in <i>N. benthamiana</i> by PCR	Page 45
Figure 3. Demonstration of TBSV P19 suppression by GFP gene	Page 46
Figure 4. The number of GVCV genomes in 100,000 cells from qPCR	Page 47
Figure 5. The standard curve of the 159 bp shows the presence of GVCV	Page 49
Figure 6. Amplification plots curve of the 159 bp showing the presence of GVCV	Page 50
Figure 7. Dissociation curve of the 159 bp showing the presence of GVCV	Page 51

INTRODUCTION

Grapevine vein clear virus (GVCV) was discovered in Missouri and its surrounding states in 2011. It is the first DNA virus reported in the grapevine that is associated with severe disease, reduces grape yield, and damages berry quality (1) (2) (3). The reference genome of GVCV has a circular, double-stranded DNA molecule of 7,753 bp with three open reading frames (ORF) (3). The typical symptoms of the GVCV-associated disease are translucent vein clearing on young leaves, short internodes, and declining vine vigor (2). Subsequent studies indicated that grapevine aphid is a natural vector to transmit GVCV from *Ampelopsis cordata* to cultivated grapevines in vineyards (4). These studies suggest that there is a close relationship between this disease and GVCV, but more evidence is still needed to satisfy Robert Koch's postulates if GVCV is proven to be the sole causal pathogen of infection for the disease (1).

Three out of four postulates from Koch were already satisfied through a series of previous studies: GVCV was detected in all diseased plants and wild *A. cordata* (4); GVCV was introduced into a healthy grapevine through grafting and by aphids as well as the GVCV-grafted grapevines showed the same symptoms (4). But I still need more evidence for the last postulate, the same virus must be reisolated from the inoculated, diseased grapevine (1). Therefore, the objective of the experiment was to provide evidence to satisfy all of Koch's assumptions. GVCV should be introduced into healthy plants by full-length infectious clone, the full-length GVCV genome should be detected, and the same symptoms should be observed in infected grapevines.

In previous studies, graduate students Cory Keith constructed a recombinant binary plasmid containing the 1.4 length-GVCV genome (5), and student Tan Jia carried out the experiment of the GVCV infectious clone on *Nicotiana benthamiana* and Chardenol by using the 1.4 length-GVCV genome. However, the results did not meet expectations, and the infectivity

was inconsistent. It is known that virus-induced gene silencing (VIGS) is an RNA-mediated defense pathway to target invading viruses, which is a reasonable explanation for inconsistent infection of *N. benthamiana* plants by the full-length infectious GVCV clone (6). I speculated that VIGS may prevent the GVCV infectious clone from initiating efficient replication of GVCV. Therefore, I posted a central question "**How can GVCV infectivity be increased?**"

An infectious clone contains a full-length genome of a virus used *in vitro* or *in vivo* to make model experimental organisms infected (7). It has been used as the main method in this study. In addition, tomato bushy stunt virus (TBSV) P19 as a viral suppressor of VIGS was added to the previous system and the process of agroinfection (6). It has been shown that the expression of P19 with non-related plant viruses can enhance viral replication by dampening VIGS (References). The mechanism underlying P19's function can be interpreted as P19 being a strong inhibitor of VIGS that binds short interfering RNAs (siRNAs) by forming homologous dimers, which blocks the operation of the RNA-induced silencing complex (RISC), thus disabling RNA interference (RNAi) (8). For this reason, P19 is widely used to increase viral protein expression levels, but only a small amount is used to promote invasive cloning, for example, the co-agroinfiltration model of *GV3101* vectors constructed by pBin35SRBZ-CIBV and pBin35S-P19 successfully increased the efficiency of Citrus leaf blotch virus (CLBV) infectious clone (9). In this study, I reasoned that the infectivity of GVCV infectious clone could be improved or become consistent if co-infiltrate an agrobacterial strain that hosts a binary plasmid containing the TBSV *p19* gene with an agrobacterial strain containing the infectious clone of GVCV. I hypothesized that the efficiency of GVCV infectious clone's replication can be improved with the addition of TBSV P19 as a VIGS suppressor.

Therefore, the purpose of the experiment was to test whether P19 could increase the

infection efficiency/efficacy of GVCV. I designed different treatments to include with P19 or without P19 on *N. benthamiana* and 'Chardone'. Polymerase chain reaction (PCR) was used to detect GVCV in agroinfected plants, and qPCR was used to calculate the number of GVCV molecules in infected plant tissues.

LITERATURE REVIEW

Badnavirus

Molecular Characteristics. *Badnavirus* is one of the genera of plant pararetroviruses (*Caulimoviridae* family) with bacilliform virion morphology. It is a group of viruses harmful to and damaging agricultural and horticultural crops in the tropics (North and South America, Asia, Australia, Europe, and Africa), particularly taro, cocoa, black pepper, and yam (10). The genome of badnaviruses usually consists of an approximately 7.5 kbp double-stranded circular DNA molecule with three to seven open reading frames. Virions are in the bacilliform shape of around 60-900 nm long and 35 nm wide (11), and exist mainly in the cytoplasm and vacuoles of plant cells (10).

Symptomatology and Host Range. *Badnaviruses* infect many types of plants, including monocotyledons and dicotyledons, and cause economic losses ranging from 10% to 90% to various host crops in subtropical and tropical regions (10). The symptoms caused by badnaviruses are mild to moderate according to different hosts and varieties, virus types, and environmental conditions. Disease complications result in crop quality decline, vigor and yield reduction, and economic losses (10). The main symptoms include pronounced chlorotic and necrotic lesions on leaves of banana plants affected by Banana streak virus (12); severe yellow mosaic on *Bougainvillea spectabilis* leaves caused by Bougainvillea vein banding-associated badnavirus (13); swelling root and stem, mosaic and leaf chlorosis in *Theobroma cacao* caused by Cacao swollen shoot virus (14); Citrus mosaic disease in *Citrus* (sweet orange, Rangpur lime, acid lime, pummelo) caused by Citrus yellow mosaic badnavirus (15); vein clearing, chlorotic flecks, chlorotic mottling along veins and characteristic curling of leaves in *Pineapple* caused by Pineapple bacilliform comosus virus (11).

Genome Organization and Replication. All pararetroviruses use RNA intermediates to replicate their double-stranded DNA through reverse transcription and replication. Generally, the replication process of cauliflower mosaic virus (CaMV), a type member in the Caulimoviridae family, has been used as a model to learn and study viral replication in this family (Hohn T, 2013). CaMV is an 8 kbp circular double-strand DNA virus with two promoters 35S and 19S. The 35S promoter with a duplicated enhancer drives the transcription of pre-genomic RNA/polycistron mRNA, so it is commonly used in the transcription of DNA molecules to make RNA transcripts. The 19S promoter drives the transcription of another RNA transcript that encodes the transactivator (16, 17). As with the core promoters, two other major enhancer regions are found: region A (-90---46) for leaf tissue expression, and region B (-343---90) for root system expression (17). In addition, Rice Tungro Bacilliform virus (RTBV), promoters in downstream sequences also have strong transcriptional activity, even comparable to CaMV 35S promoters, and these downstream sequences also activate CaMV 35S promoters (18).

Pararetroviruses synthesize repeated sequences at both ends of virus RNA during replication, known as terminal redundancy which contains a polyadenylation signal in the repeated sequence (19). In CaMV, the significance of the location of the polyadenylation signal is that RNA polymerase skips the 5' end of the sequence to recognize the 3' end of the polyadenylation signal during the synthesis of full-length RNA. In addition, sites near the start of transcription inhibit polyadenylation signaling and thus RNA 3'-end processing (20).

For pararetroviruses, the number of viral proteins is increased by the selective alternative splicing in the transcription process (17). For instance, the transient expression assay based on CaMV genome construction revealed that open reading frame I (ORF I) splicing factor was used in the lead sequence of CaMV 35S RNA and three additional splicing donor sites within the ORF

I. The virus can produce the mRNA only after splicing the middle part of the precursor and ORF II, ORF III, and ORF IV, therefore CaMV can be effectively replicated and detected in the plant. In subsequent experiments, the deletion of the splicing factor sites made the viral mutants non-infectious, suggesting that splicing plays an important role in CaMV infectivity and viral activity (21).

Grapevine Vein Clearing Virus

Discovery. In 2004, Chardonnay grapevines (*Vitis vinifera*) showed severe virus-like symptoms for three consecutive years. The symptoms include translucent vein-clearing under sunlight, short internodes, crinkled blade, the deep green and shallow yellow mosaic pattern on leaf tissue, vine vigor declining, small clusters, and a reduction in fruit quality and quantity (2). A series of subsequent investigations revealed that more than 90% of grapevines were affected by the virus-like disease in a single vineyard. This new virus damaged plants like Chardonnay, Chardonel, Cabernet Sauvignon, Vidal Blanc, Cabernet Franc, and Riesling, the most destructive virus found in Missouri and surrounding areas (3). Later, when Chardonnay vines with translucent vein-clearing leaves were grafted as scion to healthy Cabernet Franc, Baco Blanc, and LN-33, and the same symptoms were observed on new leaves, indicating that the virus could be transmitted through grafting (2).

To study possible association of viruses with symptoms, a protein level detection ELISA and DNA level detection RT-PCR were used to detect known viruses, Grapevine leafroll-associated virus 3 (GLRaV-3), Tomato ringspot virus (ToRSV), Grapevine fanleaf virus (GFLV), Arabis mosaic virus (ArMV) in the symptomatic leaves but all tested negative for these viruses. These results suggested other viruses than those known are involved in causing the disease (2).

At that time new method for finding unknown viruses through genome sequences was developed, it is based on a phenomenon called RNA silencing (RNAi). In RNAi-mediated defense to fight against viruses, small-interfering RNAs (siRNAs) are used as guides to degrade cognate single-stranded RNA (ssRNA) and double-stranded (dsRNA) molecules and serve also as a guide for virus identification (Ding, S. W., 2007). The invading plant virus acts as an inducer of RNAi to cause a large accumulation of siRNA in the plant cytoplasm. Therefore, the type and quantity of siRNA represent the progressive degradation process of the target virus. The high-throughput sequencing of siRNA can identify the type, population structure, and genetic information of the new viruses (3).

In a subsequent study, the above high throughput sequencing technique was used to sequence the siRNA from two cDNA libraries that were built from diseased leaf tissues. Deep sequencing of siRNAs from symptomatic ‘LBC0903’ Chardonnay grapevine and asymptomatic ‘VFM411’ grapevine led to the discovery of a new virus with a double-stranded, circular DNA genome of 7,753 bp that encodes three open reading frames (ORFs), which has not been formerly reported in grapevines (3).

According to the main symptom of vein clearing, this virus was named Grapevine vein clearing virus (GVCV), which belongs to the Badnavirus genus in the family *Caulimoviridae*. It is also the first DNA virus reported in the grapevine. The discovery of the GVCV has significant implications for wine and grape production in Missouri and the neighboring region (3).

Genome Structure. In 2011, 7,753 bp circular DNA genome of GVCV-CHA with three ORFs from symptomatic ‘LBC0903’ Chardonnay grapevine was first reported (3); in 2016, the two isolates GVCV-VRU1 (7,755 bp) and GVCV-CVRU2 (7,725 bp) from wild grapevine *Vitis rupestris* were discovered. Until now, the genomes of seven GVCV isolates were sequenced that

shared 92 to 99% identical nucleotides and ranged from 7,726 bp to 7,765 bp in length: GVCV-CHA, GVCV-VRU1, GVCV-VRU2, GVCV-AMP1, GVCV-AMP2, GVCV-AMP3, GVCV-CHA2 (4, 22). The GVCV genome starts from 5'-TGGTATCAGAGCTCCAG on the positive strand, complementary to the 3'-end 12 nt of the plant tRNA^{met} sequence (3'-ACCAUAGUCUCGGUCCAA). The length of the intergenic region (IGR) varied from 883 nt to 917 nt, ORF I from 624 nt to 627 nt, ORF II from 381 nt to 390 nt, ORF III from 5,823 nt to 5,829 nt. The identical nucleotides of the intergenic region (IGR) ranged from 90.2% to 100%, ORF I from 92.4% to 100%, ORF II from 83.4% to 100%, and ORF III from 91.9 to 100% (22). Moreover, ORF II is the most variable region within a single population. In the sequencing of an increasing number of ORF IIs from different GVCV isolates, GVCV-CHA and GVCV-VRU2 had the same ORF II length of 381 nt, while the ORF II length of GVCV-VRU1 was 390 nt. This difference is due to the fact that the GVCV-VRU1 ORF II has 9 more nucleotides than GVCV-CHA and GVCV-VRU2. Where did the 9 bp come from? Was it inserted or deleted? These are the questions I ask and the reason I made ORF II the focus of subsequent genomic studies on GVCV (viral insect and graft transmission, molecular cloning, infectious cloning, etc.) (22)

Transmission of GVCV in Nature. To investigate sources of GVCV, researchers found in 2019 that 31% of wild *Ampelopsis cordata* (common name: heartleaf pepper vine) plants were infected with GVCV. After sequencing, GVCV-AMP1 was found to share 99.8% identical nucleotides with the genome of GVCV-CHA, it is inferred that this virus is likely transmitted by insects. It is known that the family *Caulimoviridae* is one of the eight plant virus families transmitted mainly by aphids. In a series of aphid transmission experiments, the single aphid from descendants of viviparous aphids acquired GVCV-AMP1 and was transferred to virus-free Chardone grapevines. After 45 days of transmission, two out of three Chardone's new leaves

showed the typical GVCV symptoms with translucent vein clearing. The GVCV genome sequence on Chardonnay transmitted by aphids was 99.5% identical to GVCV-AMP1, indicating that aphids acted as natural vectors to transmit GVCV from *A. cordata* to cultivated grapevines in vineyards (4). Continuous sample collection revealed that aphids carried identical GVCV variants in both wild and cultivated grapes, further demonstrating that aphids played a key role in the transmission of GVCV. In addition, DNA extracted from the stylet and from the body of a single aphid showed that more of the GVCV genome came from the body of the aphids. Although more research is needed to understand the roles of GVCV virions in aphids, simultaneous extraction of GVCV from stylet and body suggests that the transmission pattern of GVCV is semi-persistent (23).

Norton Grapevine is Resistant to GVCV. Graft-transmission experiments were carried out by grafting GVCV-free Norton with GVCV-infected Chardonnay for three years, and GVCV virus was not detected in all the samples no matter whether Norton was used as a scion or rootstock. GVCV was also added in the experiment of grafting virus transmission by detection of viral small RNAs (vsRNAs). With the same method, GVCV-free Norton and GVCV-infected Chardonnay were used as scions and rootstocks of each other for the grafting experiment. Compared with the susceptible plant Chardonnay, only a very small amount of GVCV vsRNAs can be transferred to Norton tissues by grafting (24). According to the conclusion of the two above grafting transmission experiments, Norton is resistant to GVCV (25).

Infectious Clone

An infectious clone is a full-length DNA clone used *in vitro* to make model experimental organisms infected. At the end of the 20th century, infectious clones of viruses emerged as a

breakthrough method that offers possibilities for the molecular study of the virus. Infectious clones of viruses have been used to understand the biological function of viral proteins and their interactions with host cells by mutation and reengineering the cloned viral genome (7). In other words, a mutated virus was produced to infect host cells so that potential functions of viral genes or segments are then unveiled (26). In addition, virus-based vectors constructed from infectious clones were designed to express therapeutic proteins. They are also used to discover VIGS components (27).

With the discovery of reverse transcriptase and the progress of recombinant DNA technology in 1978, Taniguchi T. proposed that plasmids could carry complete viral genomes and be transferred to bacteria to form infectious viruses (28). Infectious clones is considered an excellent tool for cloning full-length viral DNA and for infecting experimental plants in the last 30 years (7, 29). Brome mosaic virus (BMV) is the first plant virus successfully used for the infectious clone, in which a double-stranded cDNA molecule of BMV RNA genome was inserted in a recombinant plasmid, and then transferred to competent *E. coli* JM101 (30). After this discovery, almost all plant viruses can be built into infectious clones for functional analysis of viral proteins and genomic elements.

Agroinoculation

Agroinoculation is a method of transmitting the virus and analyzing the function of the virus genome by transferring the viral genomes I am interested into *Agrobacterium tumefaciens*' binary vector. The *A. tumefaciens* can be used as a common delivery vehicle for agroinoculation because it contains tumor-inducing (Ti) plasmids, which can naturally become cancerous in the case of plant tissue destruction (31). And at the same time, organic acids, amino acids, and

sugars secreted by damaged plant cells act as chemical inducers to promote the binding of agrobacterial cells to plant cells and modify the tumor-inducing genes with the gene of interest entering the plant nucleus (32).

Agroinfiltration is a derivative of the agroinoculation method, which is mainly used to temporarily express transgenes or fragments in plants to express the target proteins and analyze gene functions. This technology replaced the intercellular space of plants with the liquid containing *A. tumefaciens* through stomata to complete the transport of foreign genes to host plants (33). Therefore, it is widely used in the field of plant virology to study the biological functions of viral genes and proteins as well as the interactive pathways between viral proteins (34)

The efficacy of agroinfiltration depends on the spreading of bacterial cells through the plant epidermis into the interior of leaves (35). Therefore, the penetration efficiency of agrobacterial suspensions is related to the size of intercellular capacity and the arrangement of mesophyll cells in the leaves (35). Also, agroinfiltration is completed by spontaneous osmosis in the plant cell or by forced infiltration through a needle-free syringe or vacuum pump (33). Agrodrench, another innovative method, soaks the roots in agrobacterium-containing fluids (Ryu CM, 2004). Syringe infiltration is the most convenient and efficient method for analyzing genes and proteins in agroincubation. It allows multiple agrobacterial vectors to be injected into a single leaf, which was practiced in *Arabidopsis*, tobacco (36), watermelon (37), soybean (38), and pea (39).

From establishing clonal vectors to agroinfiltration of plants, there have been many difficulties in the early stage of working with infectious clones. First, early cloning difficulties of full-length viral genes are caused by presence or absence of restriction sites in vectors and viral

genes. Second, since the recombination sequence is in the final assembly, there will be clones with deletions or ‘scars’ (40). Cloning scars can reduce the survival rate and infectivity of the virus, which presents another challenge for infectious clones. Moreover, the infiltration of agrobacterial suspensions in plant tissues was not uniform. The infiltration method was complicated and time-consuming, leading to inconsistent results and the unreadable expression of infectious clones (35). The environmental stress or the increase of active oxygen produced by the oxidation burst reaction of *A. tumefaciens* after invading plant cells will lead to cell necrosis, so it is not conducive to the infectivity of infectious clones (References).

However, as time goes on, these difficulties are overcome by new technologies. For example, many virologists have been using Gateway, GeneArt Seamless cloning Kit In-Fusion, and Gibson assembly to produce efficient and successful seamless clones (40). Appropriate concentrations of antioxidant and anti-necrotic chemical additives such as lipoic acid, ascorbic acid, and acetyleugenol can improve the infectivity of infectious clones and protein expression (41). Besides, silencing suppressors such as TBSV P19 (42) and Cucumber mosaic virus (CMV) 2B (43) inhibit VIGS, they can be used to improve the infectivity of infectious clones. In addition to these new techniques and methods, the appropriate plant age, temperature, light source, leaf permeability, pH concentration of the medium, bacterial density, plant culture time, and other external environmental factors in the infection process can impact the efficiency of agroinfiltration and agroinoculation (41).

Silence Suppressor

Posttranscriptional gene silencing (PTGS) is a diverse ecosystem of organisms living alongside pathogens. Animals and plants in ancient times could survive with their immune

systems, even without vaccines and drugs (44). The PTGS is a natural weapon protecting hosts against viral infection, which uses small RNAs that are products of virus-derived double-stranded RNAs to bind and degrade viral gene transcripts (42). However, as one of the world's oldest living organisms, virus also has a remarkable ability to survive. For instance, TBSV encodes P19 protein, enhancing TBSV's ability to infect the host by inhibiting PTGS. P19 is a 19 kDa cytoplasmic protein produced by one of the three 3'-end proximal ORFs on the TBSV genome, which is entirely contained in the intercellular motor p22 gene (45).

Silence Suppressor P19. Rochon suggested that TBSV P19 was responsible for Cymbidium ringspot virus's symptoms in plants, although its biological function had not been discovered (46). TBSV P19 was proved to be an essential factor in the replication, transcription, and gene expression of TBSV in plant cell protoplasts, especially in host *N. benthamiana* and *N. cleveland* (47). Subsequent experiments showed that P19 plays a crucial role in viral infectivity. After transmitting the TBSV virus to various host plants, it induces the hypersensitivity of TBSV in resistant plants such as tobacco and causes viral symptoms in susceptible plants *N. benthamiana* and *N. cleveland*. Third, TBSV P19 has multiple functions associated with host range and symptom severity (45).

As a widely recognized potent suppressor, P19 plays a crucial leading role in the long-distance movement of the virus throughout the entire plant. Initially, P19 was thought to cause severe necrosis of host plant tissue and dysfunction of plant veins. Consequently, it was speculated that P19 enhances the efficiency of TBSV transport in the host by facilitating virus penetration into cells, thereby interfering with the plant defense system (47). Subsequently, directed mutations of several amino acids on P19 indicated that P19 can recognize and bind siRNAs and thus inhibited RNA silencing likely by sequestering viral siRNAs to prevent their

incorporation into RISC (45). Furthermore, the crystal structure of the complex between P19 of Caryophyllus Italiana ringspot virus (CIRV) and 21 nt siRNA were purified and examined. Jeffrey found that P19 recognized siRNA by interacting with siRNA's intermediate and terminal phosphorous groups with the polar residues above its substructure (Jeffrey M, 2003). Later, it was found that P19 has a strong affinity for the 21nt siRNAs (Jeffrey M, 2003). In summary, as a strong RNAi inhibitor, P19 acts by forming homodimer dicer, which binds siRNA, thereby preventing the operation of RNA-induced silencing complex (RISC) and making RNAi ineffective (8).

TBSV P19 has been used to improve the efficiency of plant virus infectious clones and increase transient protein expression levels. According to many previous studies, like Citrus leaf blotch virus (CLBV), RNA was extracted from an infected kumquat, and three overlapping cDNA fragments of the entire genome of the CLBV were obtained by RT-PCR and cloned into plasmid vector Puc35S-8.1 (48). Vives's laboratory constructed a full-length cDNA clone of CLBV gRNA, which successfully induced systemic infection of citrus host plants injected with the virus, but not of *Toona Sinensis*, *Occidentalis*, and *N. benthamiana*. After a series of experiments, they found that the co-infiltration model of *A. tumefaciens* vectors with pBin35SRBZ-CLBV and pBin35S-P19 was used successfully in infecting host plants with infectious clones. In addition, approximately 100% of *Etrog pomelo*, *N. benthamiana*, and *N. occidentalis* plants were successfully infected with viral symptoms if the plants were co-agroinfected with agrobacterial strains containing infectious clones and TBSV P19 gene. (9).

In addition to its outstanding contribution to infectious cloning, TBSV P19 can significantly improve transient protein expression efficiency. For example, Calabash yellow dysplastic virus (CYSDV), a plus-sense single-strand RNA virus, belongs to the genus *Crinivirus*

in the family Closteroviridae (49). Steel E's laboratory tried to produce antibodies by purifying CYSDV particles (50). However, due to the poor stability of virus particles, CYSDV is challenging to infect plants in large quantities to produce integral proteins (51). To overcome the virus purification difficulty, they tried clone the pBin 35SC plasmid with the green fluorescent protein (GFP) gene and the pBin 35sp⁺19 into *A. tumefaciens* strain C58C1. The inclusion of the co-infiltration of TBSV silencing suppressor P19 and CYSDV breaks some of the limitations of the prokaryotic expression system and causes these proteins to produce antibodies profitably (52).

Well-studied Infectious Clones of Grapevine Viruses

Wine grape has a high status in agricultural production as a high-return product. Nevertheless, high-quality wine depends on stable, sustainable, and healthy grape production. Grape and wine culture dates back to the Stone Age, 6,100 years ago, after the archaeological map of wine production was excavated (James, 2001), which proves that humans have thousands of years of experience in the cultivation and disease management of grapevine. It also means that humans have thousands of years to face the emergence and threat of various grapevine viruses. The wide transmission of serious grapevine viruses negatively impacts grapevine production significantly and reduces the quality of grapes.

Grapevine viruses have been studied more extensively due to advanced biotechnology in the past few decades. Infectious clone is one of the excellent tools for studying the pathological and physiological functions of grapevine viruses. A full-length DNA clone of a grapevine virus can also be used *in vitro* or *in vivo* for bioengineering (Hao X, 2021). Full-length infectious clones have been constructed successfully for grapevine vein clearing virus (GVCV) and

grapevine virus A (GVA) (53), grapevine virus B (GVB) (54), grapevine leafroll-associated virus (GLRaV-3) (55), grapevine berry inner necrosis virus (GINV) (56), grapevine algerian latent virus (GALV-NB) (57), and grapevine red blotch virus (GRVB) (58). First, the basic principle of constructing the full-length clones of the above viruses is to screen the restriction enzyme sites accurately. And then, several different viral fragments, which are PCR amplicons, undergo DNA purification and digestion and splicing together to insert a full-length genome into a plasmid and transfer the final construct into a bacterial cell.

Grapevine Vein Clearing Virus Infectious Clone. GVCV infectious clone was made by transforming a recombinant plasmid containing a 1.4-length GVCV genome into *A. tumefaciens* strain GV3101 through two vectors pCR8/GW/TOPO and vectors pGWB401 (59). The pCR8/GW/TOPO has a multiple cloning site (MCS) with three restriction sites Sal I (GTC GAC), Rsr II (CGGWCCG), and Avr II (CCTAGG) for cloning GVCV genome (59). Two PCR amplicons were used to synthesize the full-length genome, which was separately introduced into pCR8/GW/TOPO to synthesize two new plasmids, pCR8/4808 and pCR8/1179 (59). The three fragments RasII-RsrII, SalI- AvrII, and RsrII- SalI were produced by digesting the above two plasmids with three pairs of restriction enzymes. Fragment SalI-AvrII was inserted into pCR8/GW/TOPO vector to generate a new plasmid named pCR8/MCS (59). Then ligated the fragment RsrII- SalI to SalI-AvrII of the pCR8/MCS vector to create another new plasmid pCR8/RsrII-AvrII and use the same protocol to ligate the fragment RasII-RsrII to RsrII- SalI to construct the plasmid with the 1.4-length GVCV genome named "BsrGI GVCV" (Keith, 2018). Then, BsrGI GVCV was inserted into pCR8/GW/TOPO and transformed into vectors pGWB401, the Gateway-compatible binary vector with kanamycin-resistant gene to generate

"pGWB/GVCV". The last step was to introduce the pGWB/GVCV plasmid in *A. tumefaciens* GV3101 to form At-GV3101-LBC (59).

Grapevine Virus A (GVA) GVA. is the first full-length infectious clone constructed from a grapevine virus. The first is to insert two of the amplified cDNAs into the phagemid pBluescript KS, and then the viral gene from the middle of GVA is inserted into this plasmid again to form a full-length clone. Later, the pBluescript KS phagemids were cleaved by a restriction enzyme to generate a linear full-length GVA RNA transcripts plasmid. But instead of transferring the phagemids into bacterial cells as is done today with infectious cloning, the linear plasmid is used as a template for making grapevine virus A transcript by T7 RNA polymerase *in vitro* in a tube. The *in-vitro* RNA molecules, equivalent to grapevine virus A RNA genome, were rubbed directly onto the epidermal cells of *N. benthamiana* and *N. clevelandii*. Grapevine virus A replicated and propagated in the host plants (53).

Grapevine Leafroll-Associated Virus-3 (GLRaV-3). Five overlapping cDNA fragments were assembled into the full-length GLRaV-3 genome that was cloned into pLA41, a pUC119-based vector. These individual cDNA clones containing partial fragments are linked multiple times by adjacent and shared endonuclease sites, eventually connecting to the pLA41 plasmid between Nco I and Sma I restriction sites. Furthermore, the 35S promoter from CaMV was ligated to the 5' ends of the full-length cDNA clone of GLRaV-3 and then ligated into the binary vector pCAMBIA1380. The result plasmid pCam: LR3Full-Length containing the full-length GLRaV-3 cDNA was transferred to *A. tumefaciens* EHA105 (55).

Grapevine Algerian Latent Virus (GALV-NB). The two fragments of GALV-Nf with T7 promoter were cloned in the pUC57 vectors to build the intermediate T7-GALV-Nf vector, a full-length clone. And it was then ligated into a multiple cloning site (MCS) with a 26 bp

polylinker with CaMV 35S promoter upstream of the GALV-Nf full-length genome to form vector T7-MCS-GALV-Nf. The above plasmid was digested and ligated into the pK7WG2 plasmid as the second vector and transferred to *A. tumefaciens* EHA105 (57).

Grapevine Red Blotch Virus (GRBV). Full-length GRBV viral genomes of two different variants (NY175ab and NY358) were cloned into one vector by a rolling circle amplification (RCA) (58). The RCA products were then digested to obtain the entire length of the virus fragment and cloned into a pUC19 plasmid. After synthesizing this bitmer construct, the final step was to migrate the bitmer construct pUC19 plasmid to *A. tumefaciens* strain GV3101 to build the full-length clone (58).

METHODS

Nicotiana Benthamiana Plants

Nicotiana benthamiana is not only susceptible to distinctive viruses but can also reproduce easily and in large quantities for experimental research within a short time (60). At least 14 *N. benthamiana* plants were required for one experiment (12 for the experiment and 2 for extra replacement). *N. benthamiana* seeds were soaked in distilled water for 48 hours, sprinkled on the soil surface in pots, and then covered with plastic wrap for 48 hours. All seedlings were grown under a 16 h light/8 h dark photoperiod at room temperature. After plants grew to 1.5 cm tall, they were moved to a larger tray and then supplied ¼ teaspoon with spoon of Osmocote Smart-Release Plant Food fertilizer (The Scotts Company). At room temperature, *N. benthamiana* plants were grown under a 16 h light/8 h dark photoperiod.

Agrobacterial Strains and Treatment for Agroinfiltration

At-GV3101, At-GV3101-LBC, At-pKYLX7-P19, and At-pKYLX7-GFP are the four agrobacterial strains used for this study. The At-GV3101 strain has *A. tumefaciens* C58 background, which contains the rifampicin-resistant gene and nopaline type Ti plasmid, pMP90. At-GV3101-LBC was made by transforming *A. tumefaciens* strain GV3101 with a recombinant plasmid containing the 1.4-length of GVCV genome through two vectors, pCR8/GW/TOPO and pGWB401 (59). The At-GV3101-LBC should be detected by polymerase chain reaction (PCR) through 2 primers from GVCV to guarantee the presence of virus (Table 1). At-pKYLX7-P19 strain was made by cloning the TBSV P19 gene into the binary vector pKYLX7, which has unique multiple cloning sites (MCS), HindIII, BamHI, XhoI, PstI, SacI, XbaI, and contains the CaMV 35S promoter, along with rifampicin and kanamycin resistance genes (61). At-pKYLX7-

GFP strain has the same background as At-GV3101-pKYLX7-P19. Siemering amplified the GFP gene and cloned it into pGEM-T Easy via the XhoI-SacI or XhoI- KpnI restriction enzyme sites of pGEM-7Zf(+) (62). The vector carrying *GFP* was cloned into the MCS of the *A. tumefaciens* binary vector pKYLX7 (63).

Agroinfiltration of *Nicotiana Benthamiana* Plants

Four treatments were used to do the co-agroinfiltration in pairs. Treatment 1 includes At-pKYLX7-P19 and At-pKYLX7-GFP, in which no GVCV would be expected to be detected since neither At-GV3101 nor At-pKYLX7-GFP strain contains a recombinant plasmid that has a GVCV genome in it (Table 2). Treatment 2 includes At-pKYLX7-GFP and At-GV3101-LBC (Table 2), which are expected to contain GVCV in some co-agroinfiltrated plants, consistent with previous results as discovered by former graduate student, Jia Tan. Treatment 2 also shows that the presence of GFP does not affect the infectivity of GVCV infectious clones. Treatment 3 includes At-GVGV3101-LBC and At-pKYLX7-P19 (Table 2), which would be expected to contain GVCV in all or most co-agroinfiltrated plants because the P19 is expected to enhance the infectivity efficiency of the GVCV infectious clone. Treatment 4 includes At-pKYLX7-GFP and At-GV3101 (Table 2), in which no GVCV should be detected. After 5-8 days of incubation, the fluorescence of treatment 4 was compared with treatment 1 under a UV lamp. Since *P19* can promote the expression of *GFP* in the process of co-infection of *P19* and *GFP*, then the intensity of fluorescence can provide evidence of whether *P19* was an effective expression (42). At least one *N. benthamiana* plant was infiltrated for treatment 1 and three for treatment 4, and at least five *N. benthamiana* plants were infiltrated for treatments 2 and 3.

Culturing of Agrobacteria Strains

To utilize the infectious clone and conduct agroinfiltration, four agrobacterial strains At-GV3101, At-GV3101-LBC, At- pKYLX7-P19, and At- pKYLX7-GFP were cultured in 75 ml Lysogeny broth (LB). To ensure that the bacteria cultured for agroinfiltration obtain the same OD value, I cultured At-GV3101-LBC one day in advance for 48 hours with the addition of rifampicin (10 mg/ml) and kanamycin (50 mg/ml) in a flask that was wrapped in foil at 28 °C, with shaking at 230 g until OD reached 1. I incubated the At-pKYLX7-P19 and At-pKYLX7-GFP with rifampicin (10 mg/ml) and kanamycin (50 mg/ml), and At-GV3101 with rifampicin (10 mg/ml) for 24 hours in the same incubator. Agrobacteria cells were collected by centrifuging cultured suspensions in a microcentrifuge. The collected agrobacteria cells were incubated in a flask containing 50 ml induction medium (IM) in the dark at room temperature for at least 24 hours until OD of 1 to 2. Cells were collected from the above centrifuge in a flask containing 20 ml IM with 10 μ l (200 μ M/ml) acetosyringone (AS), suspended in DMSO, and incubated in the dark at room temperature for 4 hours. The OD was adjusted to 1 before performing agroinfiltration.

Agroinfiltration of *Nicotiana Benthamiana* Plants

Watering of *N. benthamiana* plants was discontinued two days before agroinfiltration. The two agrobacteria strains in each of the four treatments were mixed at equal volumes to reach the final OD of 1 after 4 hours of dark incubation. Three leaves of *N. benthamiana* (4-5 weeks old) were chosen and 1 ml needleless syringe was used to gently permeate the leaves with

bacteria at the back of the leaf. After agroinfiltration, all the co-agroinfected *N. benthamiana* plants were grown at room temperature at a 16 h light/8 h dark photoperiod.

DNA Extraction from *Nicotiana Benthamiana* Leaves

Two and four weeks after agroinfiltration, DNA was extracted from tissues of upper, non-infiltrated leaves using Synergy™ 2.0 plant DNA Extraction Kit. I first extracted DNA from *N. benthamiana* leaves of treatment 1 and treatment 4. Subsequently, treatment 2 and treatment 3 with the full-length GVCV genome were then sampled for extracting DNA. Finally, two infiltrated leaves were randomly selected from treatment 2 and treatment 3 in order to avoid cross-contamination between treatments.

During the DNA extraction from *N. benthamiana* leaves, 90 mg of upper leaf tissue and 500 µl of plant homogenization buffer were added to the homogenization tube and the homogenizer was set up to break the leaves evenly at 400 g for four cycles of 30 seconds each with 30 seconds pause between cycles. The homogenate was put into the centrifuge at 13,000 g for 5 minutes. The supernatant was transferred into a tube containing 5 µl RNase A and incubated at 37 °C for 15 minutes to remove RNA molecules in the supernatant. Isopropyl alcohol of 70% of the total supernatant volume was then added to the tube and shaken thoroughly to bind and precipitate DNA. Isopropanol and supernatant were incubated at room temperature for 15 minutes and then filtered and removed from DNA by one minute centrifugation at 9,000 g through silica spin columns. The DNA was washed with 70% ethanol in the same silica tube for removing salt ions by one minute centrifugation of 9000 g twice. The empty tube was centrifuged at 13,000 g for 3 minutes to remove excess ethanol from the filter. The filter was transferred to a new 1.5 ml tube. The lid remained kept open for 15 minutes to let

ethanol evaporate. The DNA was collected by centrifugation for 1 minute at a speed of 9000 g after 75 µl of distilled water at 50 °C was carefully and slowly added to the filter tube and incubated for 5 minutes. The concentration and purity of DNA were determined by NanoDrop microvolume spectrophotometer. DNA was preserved at -20°C for subsequent experiments.

Polymerase Chain Reaction (PCR)

Each time two sets of primers were used in the PCR experiment, one set of primers designed from conserved sequences of GVCV was used to detect the presence of GVCV, and one set of primers based on a 16S rRNA sequence of grapevine was used to assess the quality of grapevine DNA. The primers 1101F and 1935R (1101F: 5'-CTGAAAGGTAGATGTCCACG-3' 1935 R:5'-GCCACGTGGACATCTACCTT-3'), 5044F and 5387R (5044F: 5'-ATTCCAGCCTCTTGCGCAG-3' 5387R: 5'-TCATTCCCTGCGAGGATCAT-3') are primers specifically for detecting GVCV virus while the 16SF and 16SR (16SF: 5'-TGCTTAACACATGCAAGTCGGA-3', and 16SR: 5'-AGCCGTTTCCAGCTGTTGTTC-3') are the primers amplifying 105 bp of grapevine 16S rRNA gene (Table 1).

The primer set 5044F and 5387R for amplifying a 344 bp amplicon of GVCV and the primer set 16SF and 16SR for a 105 bp amplicon of grapevine 16S rRNA are the primary detection primers in PCR. The reagents and concentrations are: 16.15 µl H₂O, 5 µl 12.5mM Buffer, 0.5 µl 0.25mM dNTPs, 0.3 µl 0.25 mM 16SF, 0.3 µl 0.25 mM 16SR, 0.75 µl 0.25 mM 5041F, 0.75 µl 0.25 mM 5387R, 0.25 µl Taq, and 1 µl 20 ng/µl sample of DNA. Then the tubes were set up in the 96 wells thermal cyclers with the initialization step at 95 °C 1 minute; the denaturation step at 95 °C 15 seconds, the annealing step at 57 °C 15 seconds, and the elongation step at 72 °C 25 seconds of cycled 35 times; and extension step at 72 °C for 5 minutes.

To further confirm the positive results, the primer set 877F and 1866R was used for PCR to amplify the ORF II region. For the 990 bp and 16S amplification, I prepared the reaction in a 0.5 ml tube as below: 16.25 μ l H₂O, 5 μ l 5x Buffer, 12.5mM 0.25mM dNTPs, 1 μ l 0.25 mM 877F, 1 μ l 0.25 mM 1866R, 0.25 0.25mM μ l Taq polymerase, and 1 μ l 20 ng/ μ l sample of DNA. Then the tubes were set up in the 96 well thermal cyclers with the initialization step at 95 °C 1 minute; the denaturation step at 95 °C 30s, the annealing step at 57 °C 15s, and the elongation step at 72 °C 1 minute at cycled 35 times; and extension step at 72 °C for 5 minutes.

Quantitative Polymerase Chain Reaction (qPCR)

qPCR should be used as a secondary screening, and the number of virus genomes in the infected samples should be calculated by the standard curve to provide accurate and quantitative data (64). The primers 402F and 560R were designed to amplify a 159 bp fragment of GVCV for qPCR. Each *N. benthamiana* plant DNA of treatment 2 and treatment 3 in all experiments and one random *N. benthamiana* DNA of treatment 1 and treatment 4 were tested. The MxPro-Mx3005P (standalone) SYBR Green was used for conducting the qPCR and set up by ROX and SYBR fluorescence data with ROX reference dye. The reaction of 159 bp of amplification in the optical tube was followed: 0.25 μ l 40x Yellow Sample Buffer, 5 μ l SYBR Green Master Mix, 0.5 μ l 402F, 0.5 μ l 560R, 3.4 μ l H₂O, and 1 μ l sample of DNA. Then the tubes were set up in the Agilent Stratagene MX3005P qPCR Machine with the initialization step at 95 °C for 10 minutes in segment 1; the denaturation step at 95 °C for 30 seconds, the annealing step at 55 °C for 30 seconds, elongation step at 72 °C for 30 seconds cycled 40 times in segment 2; denaturation step at 95 °C for 1 minute, annealing step at 55 °C 30 seconds, and elongation step at 95 °C for 30 seconds of cycled once in segment 3.

Standard Curve

Sample Selection. In addition to the standard curve for GVCV, the housekeeping gene 18S, which can be expressed stably even in *N. benthamiana* infected with the virus, was also used for qPCR standard curve making. Ct (threshold period) is the intersection of the threshold line and amplification curve. It means that the gene fragment reaches the threshold in the first amplification cycle, so it can reflect the relative measure of target concentration in PCR. The smaller the Ct value, the higher the concentration of the starting gene. Under the negative result of treatments 1 and 4, Ct values of all samples from treatments 2 and 3 were evaluated to select the three samples with the smallest Ct values.

Gel Purification. The standard curve was made by using a 159 bp fragment of the GVCV genome in eight different concentrations. The 159 bp fragment was purified from agarose gel. Firstly, the 159 bp fragment was amplified by PCR with a high-fidelity enzyme and separated on an agarose gel. A slice of agarose gel containing the fragment was cut out under a UV lamp and weighed. A binding buffer was added with three times the volume of the gel slice and incubated at 50° C for 10 minutes until all the gel was dissolved. The solution was transferred to the collection tube and centrifuged at 9000 g for 1 minute. A 750 µl wash buffer was added and centrifuged for 9000 g for 1 minute. The collection tube without a solution was centrifuged at 13000 g for 3 minutes to remove excess ethanol. The silica filter tube was transferred to a 1.5 ml microcentrifuge tube and air-dried for 15 minutes to volatilize the extra ethanol. The DNA was collected with 15 µl of distilled water by incubation at 50 °C for 5 minutes, and centrifuged for 1 minute at a speed of 9000 g. The concentration and purification of

DNA were measured by NanoDrop microvolume spectrophotometer. DNA was cryopreserved at -4°C for subsequent experiments and cryopreserved permanently at -80°C.

Sensitivity and Efficiency of the qPCR Assay. Primers designed for the GVCV-specific 159 bp DNA fragment were used to perform qPCR on all samples of the 6 experiments. To build a standard curve, the 159 bp and 18S fragments from conventional PCR were purified, and their concentrations and the number of molecules were calculated. For the sample to be tested, one sample was randomly selected from treatment 1 and treatment 4 in the 159 bp qPCR screening. The three samples with the smallest Ct value were selected, and the standard curve of qPCR was used to calculate the number of GVCV and 18S molecules from treatment 2 and treatment 3.

The qPCR Standard Curve. q PCR standard curve is used to express Ct values expressed by different DNA concentrations through several different dilutions of DNA templates. A computer program that uses a standard curve to measure the DNA sample automatically converts the Ct value to the number of target DNA molecules.

The 8 different dilutions of DNA fragments were calculated. An online calculator was used to determine the molecular weight of 159 bp GVCV-specific fragment and 18S rRNA-specific fragment (<https://molbiotools.com/dnacalculator.php>). The number of 159 bp and 18S fragments per gram was calculated by the following formula: Number of copies ($\text{ng} \times [6.022 \times 10^{23}] / (\text{length} \times [1 \times 10^9] \times \text{weight})$). The 6.022×10^{23} above is Avogadro's number, which is used for describing the number of constituent particles per mole of a gram, the length is the length of DNA fragment in the unit of base pairs, and the weight is the molecular weight of 159 bp. The final result was multiplied by 1×10^9 to convert nanograms to grams.

Using the 159 bp DNA fragment to build the standard curve, the purified 159 bp fragment concentration was diluted 8 times from 2×10^7 molecules per microliter, followed by 10-fold continuous dilutions to 2 molecules per microliter. In each qPCR setup, samples of the above eight dilutions of DNA were added to develop standard curves. In addition, three DNA samples from treatments 2 and 3 and one sample from treatments 1 or 4 were run in the same qPCR in triplicate. The MX3005P (standalone) SYBR Green was used for conducting the thermal cycling and set up by ROX and SYBR fluorescence data and ROX reference dye. The reaction of 159 bp of amplification in the optical tube is as follow: 0.25 μ l 40* Yellow Sample Buffer, 5 μ l 12.5 mM SYBR Green aster Mix, 0.5 μ l 0.25 mM 402F, 0.5 μ l 0.25 mM 560R, and 5 μ l 20ng/ μ l sample of DNA. The tubes were then placed in an MX3005P qPCR apparatus and amplified at the same time and temperature as in the previous qPCR screening step.

Same as the standard curve of 159 bp, using the 18S DNA fragment to build the standard curve, the purified 159 bp fragment concentration was diluted 8 times from 2×10^7 molecules per microliter, followed by 10-fold continuous dilutions to 2 molecules per microliter. In each qPCR setup, samples of the above eight dilutions of DNA were added to develop standard curves. In addition, three DNA samples that were extracted from treatments 2 and 3 and one sample that was extracted from treatments 1 or 4 in the same qPCR template and tested in triplicate. The amplification reaction protocol of 18S was established in the same method as the standard curve of 159 bp. Then the tubes were set up in the Agilent Stratagene MX3005P qPCR Machine with the initialization step at 95 °C for 10 minutes in segment 1; denaturation step at 95 °C for the 30s, annealing step at 55 °C for 30 seconds, and elongation step at 72 °C for 30 seconds cycled 40 times in segment 2; denaturation step at 95 °C for 1 minute, annealing step at 55 °C 30 seconds, and elongation step at 95 °C for 30 seconds for one cycle of segment 3.

RESULTS

Testing Infectivity of GVCV Infectious Clone on *Nicotiana Benthamiana* by PCR

At-GV3101, At-GV3101-LBC, At-pKYLX7-P19, and At-pKYLX7-GFP are four agrobacterial strains to test the hypothesis in this experiment. The At-GV3101 strain has an *A. tumefaciens* C58 background. At-GV3101-LBC was made by transforming *A. tumefaciens* strain GV3101 with a recombinant plasmid containing 1.4-length of the GVCV genome. The plasmid from At-GV3101-LBC was sequenced to verify the correctness of the GVCV genome sequence. At-pKYLX7-P19 strain was made by cloning the TBSV P19 gene into the binary vector pKYLX7 (Adhab, M., 2019). At-pKYLX7-GFP strain contains a recombinant plasmid in which the GFP gene was cloned into the *A. tumefaciens* binary vector pKYLX7 (Schardl et al. 1987). Both At-pKYLX7-P19 and At-pKYLX7-GFP were supplied by Dr. James Schoelz from the University of Missouri.

The four treatments were performed by infiltrating agrobacterial strains in pairs into *N. benthamiana* plants (Table 2). All the co-infiltrated *N. benthamiana* plants for each experiment were grown for weeks to allow replication of the infectious clone and to observe symptoms. Two and four weeks after agroinfiltration, the total DNA was extracted from the top fresh leaves. PCR was performed to detect GVCV. In the PCR detection, the 105 bp 18S rRNA from the plant genome was used to check the quality of extracted plant DNA. At least two sets of primers that were designed from the GVCV genome were used for detecting GVCV genome. GVCV-specific primers were designed based on the GVCV-CHA reference genome sequence.

To exclude the possibility that GVCV was detected as a result of the movement of agrobacterial cells that carry the GVCV infectious clone from the agroinfiltrated site to the top of the plant by vascular tissues, but not as a result of GVCV replication in the top leaves, I designed

one primer based on the plasmid sequence (M13), and the other is designed on the GVCV-CHA reference genome (4804R) (Table 1). A DNA fragment was expected to be detected if the agrobacterial cells were transferred to the top leaves by these backbone test. The results showed that two GVCV-specific fragments (344 bp and 672 bp) were detected in the top leaves (Figure 2A), but the DNA fragment covering part of the plasmid vector was not detected (Figure 2B). It is concluded that GVCV replicated in the top leaves.

I conducted six replicates of the experiment using a total of 88 plants. In treatment 2 when plants were co-agroinfiltrated by bacteria At-GV3101-LBC and At-GV3101-GFP (Table 2), 25 out of 30 plants were infected by GVCV (Table 3). In treatment 3, plants were co-agroinfiltrated by At-GV3101-LBC, and At-GV3101-P19, 27 out of 31 plants showed GVCV positive (Table 3). In total, 52 of the 61 plants co-inoculated with At-GV3101-LBC were successfully infected, strongly supporting that GVCV replicated in *N. benthamiana* after agroinfiltration.

The results suggest that the addition of P19 may increase the infectivity of the GVCV virus; however, it was difficult to quantify the difference in the quantity of GVCV DNA molecules between treatment 2 and treatment 3. Additional tests were needed for further comparison.

Demonstration of TBSV P19's Effect on GFP Expression in *Nicotiana benthamiana*

Treatments 1, 2, and 4 contained a GFP gene among the four treatments. The GFP gene produces a GFP from the jellyfish *Aequorea victoria*, which shows bright green fluorescence to the naked eye when exposed to blue and ultraviolet light fields (65). Because of its high visibility and efficient emission of internal fluorophores, GFP was used to observe the impact of TBSV

P19 protein on gene silencing in this experiment. TBSV P19 was shown to be a suppressor of the gene silencing (42). Therefore, by comparing the fluorescence intensity of GFP in treatment 1 with P19 and treatment 4 without P19, we can assess whether TBSV P19 is functional in suppressing gene silencing. Figure 3A was taken from plants that were agroinfiltrated with agrobacterial strains of At-pKYLX7-P19 and At-pKYLX7-GFP; Figure 3B was taken from plants that were infiltrated with agrobacterial strains of At-GV3101 and At-pKYLX7-GFP. Under the same ultraviolet light and the same plant age, the fluorescence brightness on the plants under treatment 1 is stronger than under treatment 4. This observation suggested that TBSV P19 expressed in At-pKYLX7-infiltrated cells can suppress virus-induced gene silencing.

Analysis of GVCV Genome Molecules in Agroinfiltrated *N. benthamiana* by Real-Time Quantitative PCR

Real-time quantitative polymerase chain reaction (qPCR) is a method that can be used to quantify DNA molecules compared to the results obtained by gel electrophoresis in an ordinary PCR (66). Results from PCR assays indicated that GVCV replicated in *N. benthamiana* plants that were agroinfiltrated by the infectious clone. However, it is difficult to know if TBSV P19 can improve the efficiency of GVCV infection by conventional PCR assays. Therefore, qPCR was used to quantify the GVCV genome number and the number of 18S rRNA genes expressed in the same plant tissue. The purpose of qPCR in this experiment was to compare the GVCV genome number of GVCV-positive samples between treatment 2 and treatment 3.

Based on the stand curve (Figure 4), constructing a standard curve in qPCR is essential for will accurately calculating the number of GVCV genome molecules, and also ensuring the detection sensitivity. Standard curves were prepared by diluting eight gradients of known

quantities of molecules in a tenfold decreasing manner (Figure 5). GVCV molecules and 18S rRNA fragment numbers were always calculated using the standard curves of the eight gradients in subsequent sample testing, with three replicates of each diluent. Excluding the lowest and highest concentrations, the standard curves calculated from samples with the middle six concentrations had higher R^2 and efficiency (Figure 4: $R^2=0.998$, Efficiency: 105.6%). Dissociation curve of the 159 bp showing the presence of GVCV in *N. benthamiana* by qPCR (Figure 6).

The primer set for amplifying a GVCV-specific 159 bp DNA fragment and the primer set for an 18S rRNA-specific DNA fragment from *N. benthamiana* were used in qPCR on all samples from treatment 2 and treatment 3 along with mock-inoculated samples to determine molecule numbers present. The number of molecules of GVCV can be accurately calculated when normalized by the number of 18S rRNA fragments detected in the same plant tissues. The number of 18S rRNA fragments is converted to one million as the denominator to calculate the average number of GVCV genomes per million of 18S rRNA molecules for comparison between the two treatments. Also, this is accomplished using serial dilutions of known quantities of DNA to create a standard curve for GVCV 159 bp and 18S. In four out of six treatments, treatment 3 had a greater average of 159 bp/18S rRNA than treatment 2 (Figure 4). By using Fisher's LSD multiple-comparison test, there was no statistical difference in the GVCV genome molecules between treatments 2 and 3 in experiments 3 and 6, in experiment 5 the difference is significant only at $\alpha=0.1$. Therefore, it is concluded that TBSV P19 does not improve the efficiency of this GVCV infectious clone under the conditions in this thesis project.

DISCUSSION

In 2001, a newly discovered virus was named Grapevine vein clearing virus (GVCV) in the Midwest of the United States. The associated symptoms are translucent vein-clearing, short internodes crinkled the blade, the dark green and yellow mosaic pattern on leaf tissue, and vine vigor declining (3). All of these symptoms cause damage to grapevine leaves and also lead to a reduction in fruit quality and quantity (Figure 1). The symptoms are speculated to be caused by GVCV (3). However, experimental evidence is still required to satisfy Robert Koch's postulates to prove that GVCV is the sole infectious agent of the disease. One last assumption needs to be proven: "The virus should be identified as the original one, which can be reisolated from the diseased host" (1).

As one approach to fulfill Koch's postulate, viral infectious clones are used as a tool by cloning the full-length viral genome into a bacterial plasmid and transferring it to agrobacterial strains for agro-infecting plants. A GVCV infectious clone was constructed by former graduate student Cory Von Keith, and experiments for testing the infectivity of the GVCV infectious clone were conducted by former graduate student Jia Tan. After repeated experiments, they still could not obtain consistent results to prove that infectious clones can infect *N. benthamiana*.

VIGS is an RNA-mediated defense pathway to target invading viruses, which could explain the phenomenon of inconsistent results from the infectious clone. However, some viral proteins as a helper to protect the virus from degradation by the plant immune system, can increase the efficiency of the virus genome replication and thus is defined as a suppressor of VIGS (6). In this project, P19 is a VIGS suppressor encoded by Tomato bushy stunt virus (TBSV) and is thus used to complete Koch's postulates. The P19 protein prevents siRNAs from

degrading the virus by binding to short interfering RNAs (siRNAs) (8). In addition, *N. benthamiana* can continuously be infected by almost all plant viruses and thus was selected as a model plant for this study (60).

GVCV-specific DNA fragments from four treatments were detected by conventional PCR, which determines if GVCV is presently based on the DNA size compared with the marker. Two primers from GVCV and one set of primers for the 18S rRNA gene were used for detecting GVCV by PCR. In 6 out of 6 repeated agroinfiltration experiments, GVCV-specific fragments were detected (Table 3). In addition, 83% of *N. benthamiana* were infected by GVCV in treatment 2; 87% of *N. benthamiana* were infected by GVCV in treatment 3 (Table 3). These results confirmed that At-GV3101-LBC can initiate infection of *N. benthamiana* by GVCV. And also, the number of successfully infected plants by GVCV with the inclusion of TBSV P19 in treatment 3 was higher than that without TBSV P19 in treatment 2. However, this difference in the percentage of infections is not statistically significant. Therefore, real-time quantitative PCR was used to evaluate the impact of TBSV P19 in this project.

In qPCR assays, a smaller Ct value indicates a higher initial concentration of original GVCV DNA. In 83% of experiments, the average Ct value of 159 bp in treatment 3 was smaller than that in treatment 2. 66% of the average DNA copy number of 159 bp /18S rRNA was higher in treatment 3 than in treatment 2. From these data, it can be concluded that the addition of P19 in most samples increased the GVCV genome number of plants infected by At-GV3101-LBC. Unfortunately, due to the precision of qPCR, the number of samples obtained was small, and the variation of the data obtained by qPCR was large. There are no statistically significant differences in Fisher's LSD multiple-comparison test between treatment 2 and treatment 3 in

experiments 3 and 6. But in experiment 5 the log-transformed data between treatments 2 and three would be significant.

The reason for no statistical difference between the two treatments was that the individual sample quantity differences in each treatment were large, which resulted in a large standard deviation for comparison between the two treatments. Factors that cause excessive standard deviation of the two treatment samples include plant culture, agroincubation, DNA extraction, and the process of the qPCR standard curve. In the growing environment of plants, plants of the same age were used for the agroincubation. But even at the same age, the plants do not totally have the same growing situation. Although it is difficult to control the growth of plants, in view of this factor, more extra plant samples are needed in future experiments to ensure that there is room for plant selection in agroinfiltration. And also, keeping recording the same watering time, frequency, and volume will also make it easier to control the plant's growing environment. For the incubation of all the bacteria, the different room temperatures for the last step of the bacteria incubation in IM, and the ratio of two bacteria mixing according to the promoter in the plasmid are all factors that need to be considered. Also, since p19 can affect older plants more, selecting older plants for agroincubation operation is also the plan for future experiments (8). The same DNA extraction kit was used for plant DNA extraction, and treatments 2 and 3 were extracted two weeks together after agroinfiltration. Perhaps to avoid cross-contamination, samples of treatment2 and 3 could be extracted separately on the same day in future experiments.

According to the standard curve and normal standard deviation in treatment 2, the technical operation can be ruled out. The reason for the large standard deviation in treatment 3 can be from the large standard deviation in plant ribosome RNA 18S. Since P19 can disturb the normal cell life (67). The mechanism of P19 is that P19 can combine the siRNA to protect the

virus be degraded by siRNA. But at the same time, the P19 also will combine the microRNA which is the host RNA, and play the important role in cell life.

The shortcomings of the experimental design are that just 3 out of 5 plant samples were used to calculate the GVCV genome number via the process of the qPCR standard curve. The number of GVCV among three individual plants in each of the three experiments for each treatment varied largely, which caused the standard deviation to be too large to infer statistical significance. but no extra plants were used as substitutes for comparison, which leads to computational limitations. As a result, the data between the two treatments cannot be well analyzed with statistical differences. Therefore, the results can't support the conclusion that TBSV P19 is able to improve the infectivity of the GVCV infectious clones.

Although this experiment aimed to test if P19 could promote and enhance the efficiency of infectious cloning, one conclusion confirmed that GVCV infectious clone can successfully infect *N. benthamiana* plants. One future project is to infect 'Chardonel' grapevines with this GVCV infectious clone and observe if GVCV can cause similar symptoms to those on naturally infected grapevines in vineyards. This will provide final evidence proving that GVCV is the sole pathogen causing the disease. Furthermore, whether TBSV P19 can enhance the infectivity of GVCV infectious clones can also be tested on the agro-infected grapevines instead of experimental *N. benthamiana* plants.

REFERENCES

1. R. Koch, An Address on Cholera and its Bacillus. *Br. Med. J.* **2**, 453-459 (1884).
2. W. Qiu, J. D. Avery Jr, S. Lunden, Characterization of a severe virus-like disease in Chardonnay grapevines in Missouri. *Plant Health Progress* **8**, 39 (2007).
3. Y. Zhang, K. Singh, R. Kaur, W. Qiu, Association of a novel DNA virus with the grapevine vein-clearing and vine decline syndrome. *Phytopathology* **101**, 1081-1090 (2011).
4. S. M. Petersen *et al.*, A Natural Reservoir and Transmission Vector of Grapevine Vein Clearing Virus. *Plant Dis.* **103**, 571-577 (2019).
5. C. V. Keith, *Grapevine vein clearing virus : epidemiological patterns and construction of a clone* (2018).
6. M. Lange, A. L. Yellina, S. Orashakova, A. Becker, Virus-induced gene silencing (VIGS) in plants: an overview of target species and the virus-derived vector systems. *Methods Mol. Biol.* **975**, 1-14 (2013).
7. X. Hao *et al.*, Rescue of an Infectious cDNA Clone of Barley Yellow Dwarf Virus-GAV. *Phytopathology* **111**, 2383-2391 (2021).
8. K. T. Chiong, W. B. Cody, H. B. Scholthof, RNA silencing suppressor-influenced performance of a virus vector delivering both guide RNA and Cas9 for CRISPR gene editing. *Sci. Rep.* **11**, 6769 (2021).
9. M. C. Vives *et al.*, Development of a full-genome cDNA clone of Citrus leaf blotch virus and infection of citrus plants. *Mol. Plant Pathol.* **9**, 787-797 (2008).
10. A. I. Bhat, T. Hohn, R. Selvarajan, Badnaviruses: The Current Global Scenario. *Viruses* **8** (2016).
11. A. I. Bhat, Devasahayam, S., Sarma, Y. R., & Pant, R. P., Association of a badnavirus in black pepper (*Piper nigrum* L.) transmitted by mealybug (*Ferrisia virgata*) in India. *Current Science*, **84(12)** (2003).
12. C. Pasberg-Gauhl, B. E. L. Lockhart, F. Castro-Mendivil Dibos, J. C. Rojas Llanque, Banana streak virus Identified for the First Time in Peru in Cavendish Banana (*Musa AAA*). *Plant Dis.* **91**, 906 (2007).
13. V. Baranwal, M. Arya, J. Singh, First report of two distinct badnaviruses associated with *Bougainvillea spectabilis* in India. *Journal of general plant pathology* **76**, 236-239 (2010).

14. L. S. Hagen, M. Jacquemond, A. Lepingle, H. Lot, M. Tepfer, Nucleotide sequence and genomic organization of cacao swollen shoot virus. *Virology* **196**, 619-628 (1993).
15. B. K. Borah, A. M. Johnson, D. V. Sai Gopal, I. Dasgupta, Sequencing and computational analysis of complete genome sequences of Citrus yellow mosaic badna virus from acid lime and pummelo. *Virus Genes* **39**, 137-140 (2009).
16. S. N. Covey, R. Hull, Transcription of cauliflower mosaic virus DNA. Detection of transcripts, properties, and location of the gene encoding the virus inclusion body protein. *Virology* **111**, 463-474 (1981).
17. T. Hohn, H. Roehle, Plant pararetroviruses: replication and expression. *Curr. Opin. Virol.* **3**, 621-628 (2013).
18. A. Klöti *et al.*, Upstream and downstream sequence elements determine the specificity of the rice tungro bacilliform virus promoter and influence RNA production after transcription initiation. *Plant Mol. Biol.* **40**, 249-266 (1999).
19. C. M. Stoltzfus, Synthesis and processing of avian sarcoma retrovirus RNA. *Adv. Virus Res.* **35**, 1-38 (1988).
20. H. Sanfaçon, T. Hohn, Proximity to the promoter inhibits recognition of cauliflower mosaic virus polyadenylation signal. *Nature* **346**, 81-84 (1990).
21. Z. Kiss-László, S. Blanc, T. Hohn, Splicing of cauliflower mosaic virus 35S RNA is essential for viral infectivity. *Embo. j.* **14**, 3552-3562 (1995).
22. S. Beach *et al.*, Genetic and Phenotypic Characterization of Grapevine vein clearing virus from Wild *Vitis rupestris*. *Phytopathology* **107**, 138-144 (2017).
23. A. Uhls *et al.*, Grapevine vein clearing virus Is Prevalent and Genetically Variable in Grape Aphid (*Aphis illinoisensis* Shimer) Populations. *Plant Dis.* **105**, 1531-1538 (2021).
24. S. Howard, W. Qiu, Viral small RNAs reveal the genomic variations of three grapevine vein clearing virus quasispecies populations. *Virus Res.* **229**, 24-27 (2017).
25. W. Qiu, S. M. Petersen, S. Howard, North American Grape 'Norton' is Resistant to Grapevine Vein Clearing Virus. *Plant Dis.* **104**, 2051-2053 (2020).
26. V. C. Delfosse *et al.*, Agroinoculation of a full-length cDNA clone of cotton leafroll dwarf virus (CLRDV) results in systemic infection in cotton and the model plant *Nicotiana benthamiana*. *Virus research* **175**, 64-70 (2013).
27. P. Abrahamian, R. W. Hammond, J. Hammond, Plant virus-derived vectors: Applications in agricultural and medical biotechnology. *Annual Review of Virology* **7**, 513-535 (2020).

28. T. Taniguchi, M. Palmieri, C. Weissmann, A Qbeta DNA-containing hybrid plasmid giving rise to Qbeta phage formation in the bacterial host [proceedings]. *Ann. Microbiol. (Paris)* **129** b, 535-536 (1978).
29. A. I. Bhat, G. P. Rao, "Development of Infectious Clone of Virus" in Characterization of Plant Viruses. (Springer, 2020), pp. 449-463.
30. P. Ahlquist, M. Janda, cDNA cloning and in vitro transcription of the complete brome mosaic virus genome. *Molecular and Cellular Biology* **4**, 2876-2882 (1984).
31. K. Bandurska, A. Berdowska, M. Krol, Transformation of medicinal plants using *Agrobacterium tumefaciens*. *Postepy. Higieny. i. Medycyny. Doswiadczalnej. (Online)*. **70**, 1220-1228 (2016).
32. S. B. Gelvin, *Agrobacterium* and plant genes involved in T-DNA transfer and integration. *Annual review of plant biology* **51**, 223-256 (2000).
33. I. A. Chincinska, Leaf infiltration in plant science: old method, new possibilities. *Plant Methods* **17**, 83 (2021).
34. K. Leuzinger *et al.*, Efficient agroinfiltration of plants for high-level transient expression of recombinant proteins. *JoVE (Journal of Visualized Experiments)*, e50521 (2013).
35. L. Zheng *et al.*, An improved and efficient method of *Agrobacterium syringe* infiltration for transient transformation and its application in the elucidation of gene function in poplar. *BMC Plant Biol.* **21**, 54 (2021).
36. C. M. Ryu, A. Anand, L. Kang, K. S. Mysore, Agrodrench: a novel and effective agroinoculation method for virus-induced gene silencing in roots and diverse Solanaceous species. *The Plant Journal* **40**, 322-331 (2004).
37. L. Palkovics *et al.*, First Report of Bacterial Fruit Blotch of Watermelon Caused by *Acidovorax avenae* subsp. *citrulli* in Hungary. *Plant Dis.* **92**, 834 (2008).
38. K. H. Kim *et al.*, Optimization of a Virus-Induced Gene Silencing System with Soybean yellow common mosaic virus for Gene Function Studies in Soybeans. *Plant Pathol. J.* **32**, 112-122 (2016).
39. M. Kaur *et al.*, Agroinfiltration Mediated Scalable Transient Gene Expression in Genome Edited Crop Plants. *Int. J. Mol. Sci.* **22** (2021).
40. F. Pasin, W. Menzel, J. A. Daròs, Harnessed viruses in the age of metagenomics and synthetic biology: an update on infectious clone assembly and biotechnologies of plant viruses. *Plant Biotechnol. J.* **17**, 1010-1026 (2019).
41. K. Norkunas, R. Harding, J. Dale, B. Dugdale, Improving agroinfiltration-based transient gene expression in *Nicotiana benthamiana*. *Plant methods* **14**, 1-14 (2018).

42. W. Qiu, J. W. Park, H. B. Scholthof, Tombusvirus P19-mediated suppression of virus-induced gene silencing is controlled by genetic and dosage features that influence pathogenicity. *Mol. Plant Microbe. Interact.* **15**, 269-280 (2002).
43. R. Tungadi, W. Abdulkadir, N. I. Ischak, B. R. Rahim, Liposomal formulation of snakehead fish (*Ophiocephalus striatus*) powder and toxicity study in zebrafish (*danio rerio*) model. *Pharmaceutical Sciences* **25**, 145-153 (2019).
44. M. A. Ashfaq *et al.*, Post-transcriptional gene silencing: Basic concepts and applications. *J. Biosci.* **45** (2020).
45. M. Chu, B. Desvoyes, M. Turina, R. Noad, H. B. Scholthof, Genetic dissection of tomato bushy stunt virus p19-protein-mediated host-dependent symptom induction and systemic invasion. *Virology* **266**, 79-87 (2000).
46. S. B. Alam *et al.*, Targeting of cucumber necrosis virus coat protein to the chloroplast stroma attenuates host defense response. *Virology* **554**, 106-119 (2021).
47. H. B. Scholthof, K. Scholthof, A. O. Jackson, Identification of tomato bushy stunt virus host-specific symptom determinants by expression of individual genes from a potato virus X vector. *The Plant Cell* **7**, 1157-1172 (1995).
48. M. C. Vives, L. Galipienso, L. Navarro, P. Moreno, J. Guerri, The nucleotide sequence and genomic organization of Citrus leaf blotch virus: candidate type species for a new virus genus. *Virology* **287**, 225-233 (2001).
49. I. C. Livieratos, A. D. Avgelis, R. H. Coutts, Molecular characterization of the cucurbit yellow stunting disorder virus coat protein gene. *Phytopathology* **89**, 1050-1055 (1999).
50. E. Steel, I. Barker, C. Danks, D. Coates, N. Boonham, A. tumefaciens-mediated transient expression as a tool for antigen production for cucurbit yellow stunting disorder virus. *Journal of virological methods* **163**, 222-228 (2010).
51. R. Coffin, R. H. Coutts, The closteroviruses, capilloviruses and other similar viruses: a short review. *Journal of General Virology* **74**, 1475-1483 (1993).
52. O. Voinnet, S. Rivas, P. Mestre, D. Baulcombe, Retracted: An enhanced transient expression system in plants based on suppression of gene silencing by the p19 protein of tomato bushy stunt virus. *The plant journal* **33**, 949-956 (2003).
53. N. Galiakparov, E. Tanne, I. Sela, R. Gafny, Infectious RNA transcripts from grapevine virus A cDNA clone. *Virus Genes* **19**, 235-242 (1999).
54. Y. Moskovitz *et al.*, Sequencing and assembly of a full-length infectious clone of grapevine virus B and its infectivity on herbaceous plants. *Arch Virol* **153**, 323-328 (2008).

55. S. Jarugula, S. Gowda, W. O. Dawson, R. A. Naidu, Development of infectious cDNA clones of Grapevine leafroll-associated virus 3 and analyses of the 5' non-translated region for replication and virion formation. *Virology* **523**, 89-99 (2018).
56. X. Fan *et al.*, Development of a Full-Length Infectious cDNA Clone of the Grapevine Berry Inner Necrosis Virus. *Plants. (Basel.)* **9** (2020).
57. A. Lovato *et al.*, Construction of a synthetic infectious cDNA clone of Grapevine Algerian latent virus (GALV-Nf) and its biological activity in *Nicotiana benthamiana* and grapevine plants. *Virol. J.* **11**, 186 (2014).
58. L. M. Yepes *et al.*, Causative role of grapevine red blotch virus in red blotch disease. *Phytopathology* **108**, 902-909 (2018).
59. C. V. Keith, Grapevine Vein Clearing Virus: Epidemiological Patterns and Construction of a Clone. (2018).
60. M. M. Goodin, D. Zaitlin, R. A. Naidu, S. A. Lommel, *Nicotiana benthamiana*: its history and future as a model for plant-pathogen interactions. *Mol. Plant Microbe. Interact.* **21**, 1015-1026 (2008).
61. M. Adhab *et al.*, Tracing the Lineage of Two Traits Associated with the Coat Protein of the Tombusviridae: Silencing Suppression and HR Elicitation in *Nicotiana* Species. *Viruses* **11** (2019).
62. K. R. Siemering, R. Golbik, R. Sever, J. Haseloff, Mutations that suppress the thermosensitivity of green fluorescent protein. *Current Biology* **6**, 1653-1663 (1996).
63. C. L. Schardl *et al.*, Design and construction of a versatile system for the expression of foreign genes in plants. *Gene* **61**, 1-11 (1987).
64. S. C. Taylor *et al.*, The Ultimate qPCR Experiment: Producing Publication Quality, Reproducible Data the First Time. *Trends. Biotechnol.* **37**, 761-774 (2019).
65. R. Y. Tsien, The green fluorescent protein. *Annu. Rev. Biochem.* **67**, 509-544 (1998).
66. B. Thornton, C. Basu, Rapid and simple method of qPCR primer design. *Methods Mol. Biol.* **1275**, 173-179 (2015).
67. F. Qu, T. J. Morris, Efficient infection of *Nicotiana benthamiana* by Tomato bushy stunt virus is facilitated by the coat protein and maintained by p19 through suppression of gene silencing. *Mol. Plant Microbe. Interact.* **15**, 193-202 (2002).

Table 1. Primers used for detecting Grapevine vein clearing virus and assessing DNA quality
(The primer design from GenBank (accession number: JF301669.2))

Primers	Genome location and Amplicon size	Purpose	Sequence (5'-3')
16SF 16SR	<i>N. benthamiana</i> 106 bp	Amplifying a host gene for assessing DNA quality	TGCTTAACACATGCAAGTCGGA AGCCGTTTCCAGCTGTTGTTC
18SF 18SR	<i>N. benthamiana</i> 89 bp	Amplifying a host gene for assessing DNA quality	GTGACGGAGAATTAGGGTTCGA CTGCCTTCCTTGGATGTGGTA
5044F 5387R	ORF III 344 bp	PCR detection of GVCV	ATTCCAGCCTCTTGCGCAG TCATTCCCTGCGAGGATCAT
877F 1866R	ORF II 990 bp	PCR detection of GVCV	ACCAGATCGAGCTCCTTCG TCTTGCCGGTCTATGAC
402F 560R	Intergenic regions 159 bp	qPCR detection of GVCV	AGTAGGAGAGAGGACACT GGGTGCGTTCAGATCTCT
4804R	Backbone test	PCR detection of GVCV	GGAATGCATTGTGCTCGTAG

Table 2. Experimental design for testing the impact of Tomato bushy stunt virus (TBSV) P19 on the infectivity of GVCV infectious clone on *N. benthamiana*

Treatment 1	Treatment 2	Treatment 3	Treatment 4
At - pKYLX7-P19	At-GV3101-LBC	At-GV3101-LBC	At-GV3101
At-pKYLX7-GFP	At-pKYLX7-GFP	At- pKYLX7-P19	At-GV3101-GFP

At-GV3101-LBC is the agrobacterial strain containing a 1.4 genome length of GVCV.

At-GV3101 is agrobacterial strain containing an empty vector as mocked control.

At- pKYLX7-P19 is agrobacterial strain containing the TBSV P19 gene in the binary vector pKYLX7

At-GV3101-GFP is agrobacterial strain containing GFP gene in the binary vector pKYLX7

Table 3. Presence of GVCV in agroinfiltrated *N. benthamiana* plants

Expts	Treatment 1	Treatment 2	Treatment 3	Treatment 4	Date
1	0/3	4/5	4/5	0/3	1-Dec-21
2	0/3	3/5	4/5	0/3	28-Jan-22
3	0/1	5/5	5/5	0/1	13-Mar-22
4	0/1	5/5	5/5	0/1	18-Feb-22
5	0/2	4/5	5/6	0/3	13-Mar-22
6	0/3	4/5	4/5	0/3	6-Jul-22
Total	0/13	25/30	27/31	0/14	

The numerator number represents the number of GVCV-infected plants analyzed by PCR, and the denominator number represents the number of plants infiltrated with agrobacterial strains.



Figure 1. Typical symptoms of a Chardonnay grapevine that was infected by GVCV. The symptoms include translucent vein-clearing under sunlight, short internodes, crinkled blade, dark green and shallow yellow mosaic pattern on leaf tissue, declining vine vigor, small clusters, and reduced fruit quality and quantity. Photo credit Dr. Wenping Qiu.

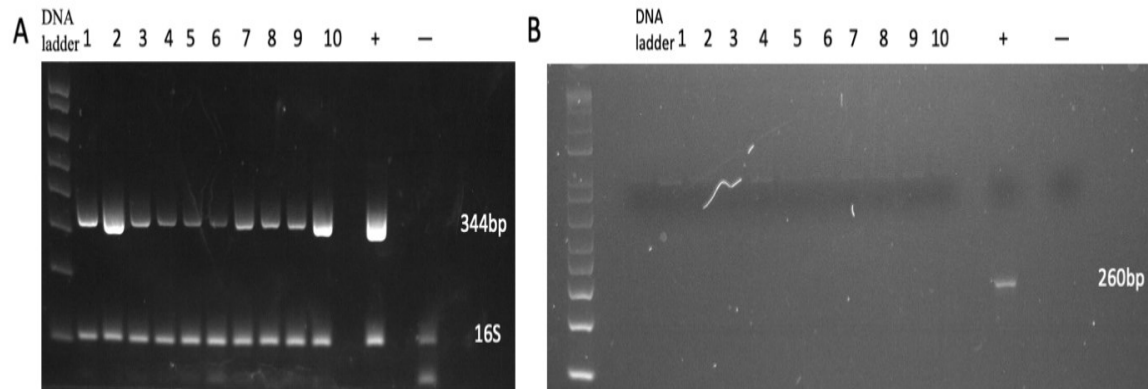


Figure 2. Testing of GVCV replication in *N. benthamiana* by PCR. Lane 1 to 5 DNA extracted from *N. benthamiana* which was infiltrated by At-GV3101-LBC and At-pKYLX7-GFP; Lane 6 to 10, DNA extracted from plants that were infiltrated by At-GV3101-LBC and At-pKYLX7-P19. +, positive control -; negative control. A) The amplified 344 bp with primer set 5044F and 5387R from GVCV. B) The backbone test (260bp) with primer set 4804F from GVCV and M13 from the backbone of the GV-3101 plasmid. The 105 bp fragment of plant 16S rRNA was used for a baseline of DNA quality.

A

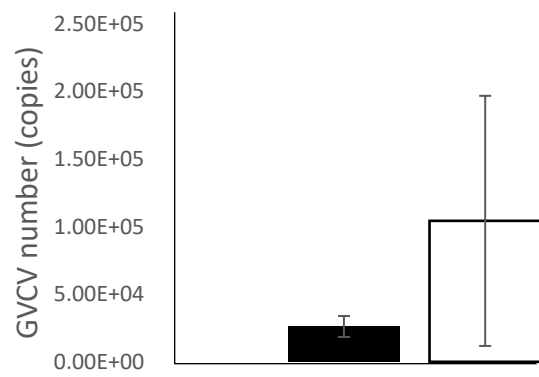


B

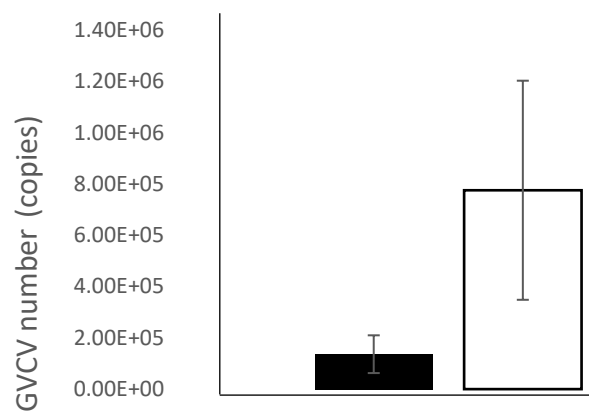


Figure 3. Demonstration of TBSV P19 suppression by GFP gene in *N. benthamiana*. Figure A is from treatment 1 which includes At-pKYLX7-p19 and At-pKYLX7-GFP; Figure B is from treatment 4 which includes GV3101 and At-pKYLX7-GFP.

A



B



C

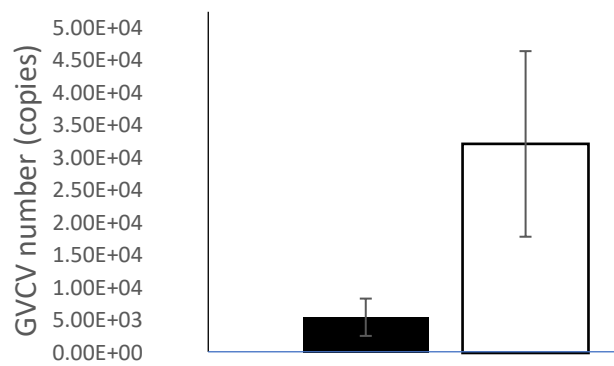


Figure 4. The quantity of GVCV genome per million 18s ribosomes. The number of GVCV genome copies per million 18S rRNA is on the Y-axis, and the two different treatment is on the x-axis. A results from experiment 3; B results from experiment 5; C results from experiment 6.

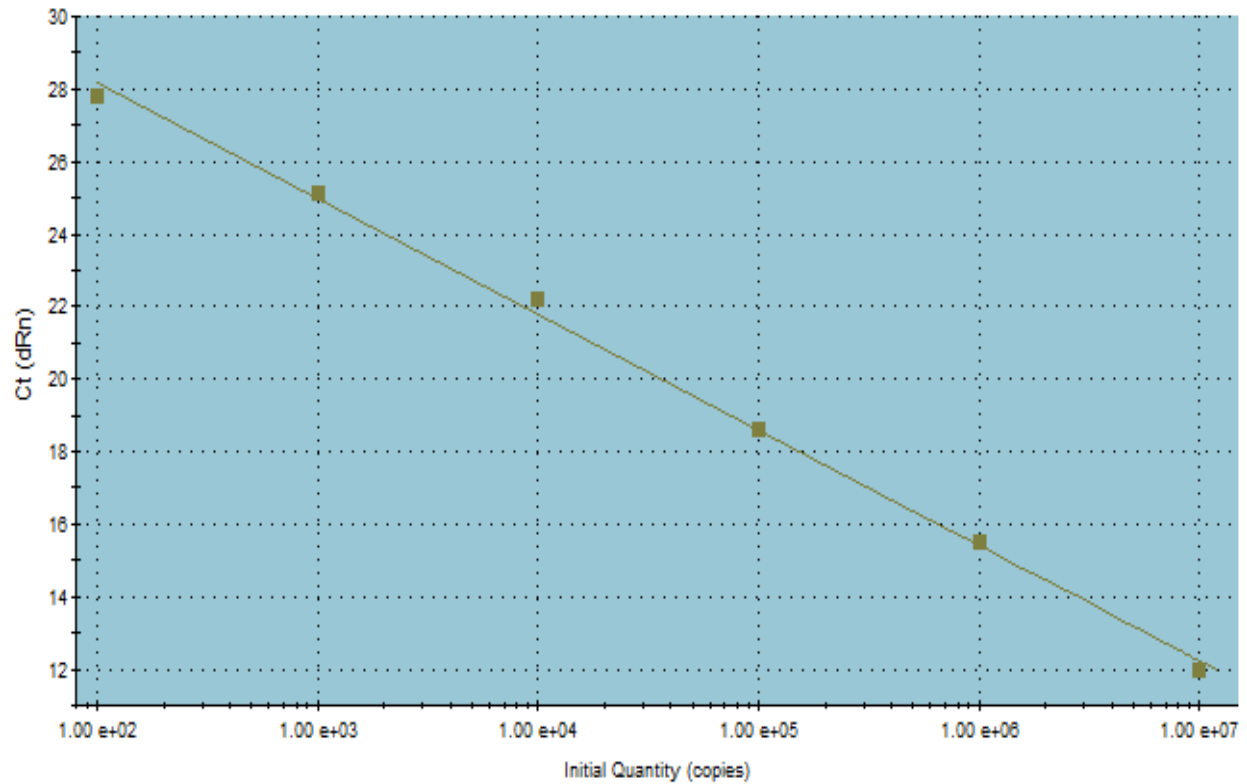


Figure 5. The standard curve of the 159 bp GVCV specific fragment in qPCR. The R^2 value (0.998) is the coefficient of correlation. The Ct values are on the Y-axis, and the quantity of log GVCV genome copies is on the x-axis. The Y-axis is calculated by the formula $Y = -3.034 \cdot \text{LOG}(X) + 34.76$. The Eff. (105.6%) is the efficiency number of qPCR by following the equation $E = (10^{-1/\text{slope}}) - 1$.

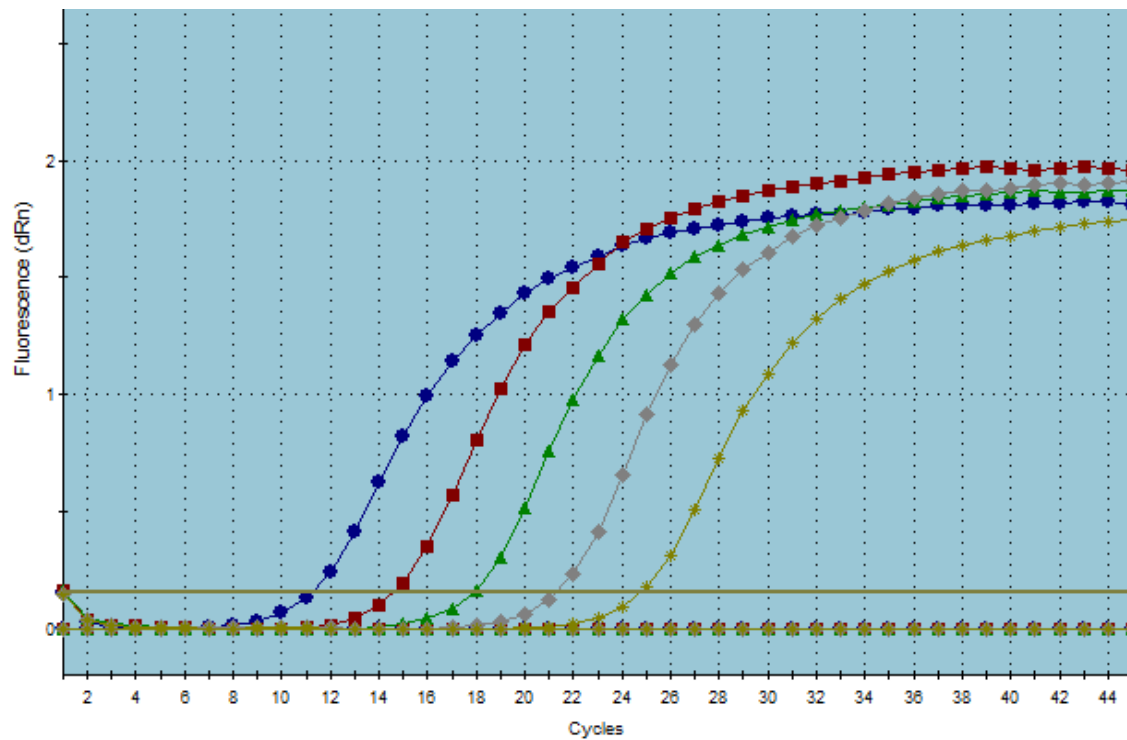


Figure 6. Amplification plots curve of the GVCV specific 159 bp DNA fragment in qPCR. The Fluorescence (dRn) is on the Y-axis, and the cycle of GVCV fragment amplification is on the x-axis. Ct (threshold period) is the intersection of the threshold line and amplification curve. It means that the gene fragment reaches the threshold in the first amplification cycle, so it can reflect the relative measure of target concentration in PCR. The smaller the Ct value, the higher the concentration of the starting gene.

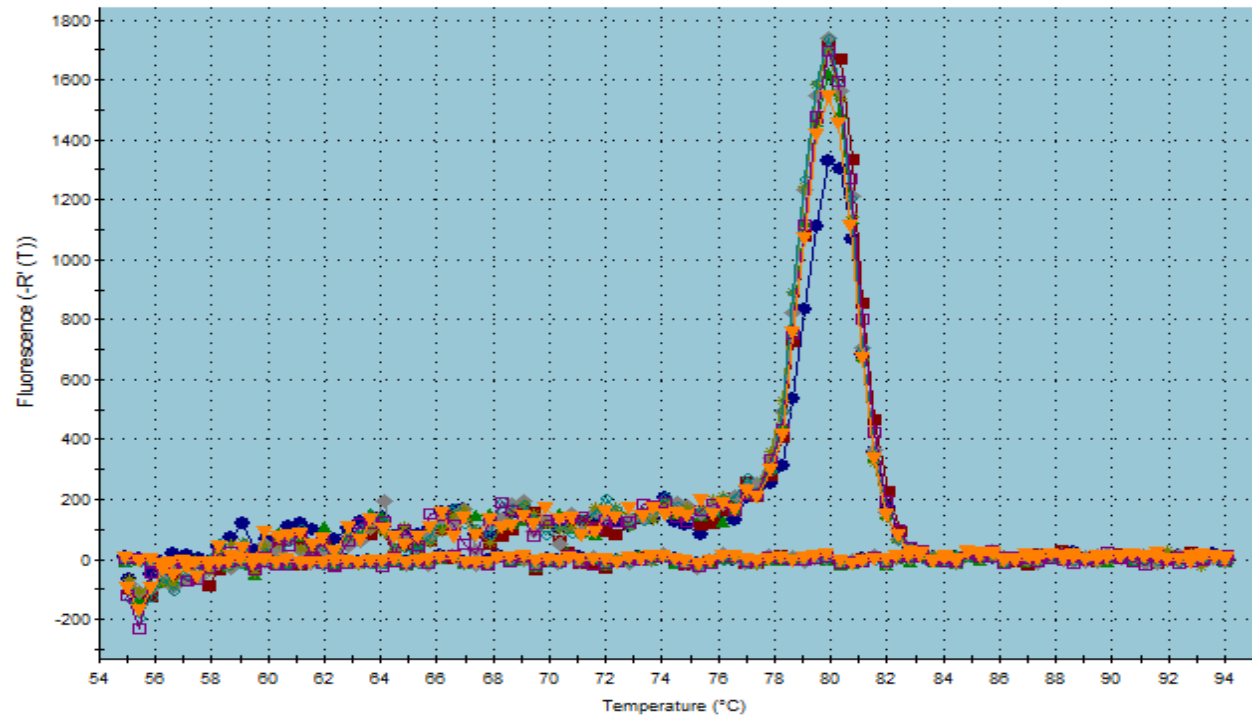


Figure 7. Dissociation curve of the GVCV-specific 159 bp fragment in qPCR. The Fluorescence(dRn) is on the Y-axis, and the temperature of GVCV fragment denaturation is on the x-axis.